Development of a near-ground novel wind energy converter

K. Calautit[1], K. Velayutham[1], and W.-G. Früh[2]

[1] Katrick Technologies, 10 Montrose St, Glasgow G1 1RE, UK

[2] Institute of Mechanical, Process and Energy Engineering, Heriot-Watt University, Edinburgh EH14 4AS, UK

Abstract. This paper investigates the performance of a novel wind energy capture system consisting of ducted oscillating aerofoils. The primary objectives of this study were to evaluate the system's ability to capture and focus wind energy, and its potential for scalability. The system is designed with modular units, each containing two aerofoils that can oscillate independently. A CFD model was developed to simulate the power extraction process, incorporating two regions within the duct to represent the action of the aerofoils. Through using an actuator volume to model the blades' inertial resistance, the thrust coefficient was calibrated, providing an accurate representation of the aerofoils' performance. The model was then placed in an open domain to evaluate the airflow dynamics and assess the available power for practical extraction. Results show that the Wind Panel design can extract up to 370 W at 12 m/s, demonstrating its strong performance in higher wind conditions, whilst producing 210 W at 10 m/s, proving its efficiency at lower wind speeds. The findings indicate that the design is a reliable, scalable, and efficient solution for sustainable energy production in varying wind environments.

Key words. Wind energy, computational fluid dynamics, porous media model, power extraction, oscillating aerofoil

1. Introduction

Utility-scale have seen tremendous and persistent rate of development and deployment, with a single device now routinely exceeding a 2 MW rating and wind farms at the scale of hundreds of MW. Alongside a convergence could be seen to the industry standard of (normally) three-bladed up-wind variable-speed pitch-controlled wind turbine rotors. In contrast to this, wind energy converters embedded in the system at the consumer or prosumer level have struggled to grow into a successful industry since the boom of building-integrated wind turbine in the 1990s which was rapidly followed by a collapse of that excitement as their performance could not meet expectations [1].

Despite that setback, research has continued exploring the full range of primary mover options, including the well-known horizontal-axis and vertical-axis rotor options [2]. This was complemented by a gradually recovery of interest in the technology by the market. Still, given the challenging wind resource at the height where these smaller turbines are deployed, any success in the market relies on a firm framework for a techno-economic evaluation of a technology option in a given operational setting [3]. One of the parts of that framework would be to determine the most appropriate technology options matching the given wind resource, for example through a morphological analysis [4]. An initial screening would then be followed by more detailed modelling of potential candidates [5].

This paper presents an investigation of such a candidate consisting of a set of ducted oscillating aerofoils. The rationale for the ducting was partly to capture and focus the wind resource but also partly to create a modular design which could be built up into a wall of energy capturing devices, for example at a property boundary, along a road, or at the perimeter of an airfield or airport runway, with an illustrative model shown in Figure 1. Each duct contains two aerofoils which could either oscillate independently of each other or coupled to work with a set phase difference.

Fig.1. Illustration of the wind energy capture device (courtesy of Katrick Technologies Ltd. [6])

This paper reports on some key steps in the design modelling of the device using Computational Fluid Dynamics (CFD). The aim of this paper is to develop an understanding of the airflow into the duct for a range of generic control strategies, with a view to design both, the aerofoil design and control and the control of the power take-off.

To achieve this, a model to represent the effect of aerodynamic forces and power train control in an abstract way within a realistic flow model of the air flow into and through the duct. One objective to work towards this is the development of that effect in a CFD module, the second is to calibrate that model against the set airflow through the duct. The third and final objective is to determine the air capture from approaching wind into the duct.

2. Methodology

Two separate CFD models were created to address these objectives. One model of a single duct was used to address the first two objectives, while the second model of a full device in a virtual wind tunnel was used for the final objective.

Given that the detailed aerodynamics of the air flow over the oscillating blades is not only very complex but also intertwined with the powertrain control, there is no advantage in trying to model that in detail. Instead, the important aspects are the interdependencies between the degree of power extraction of the air flowing through the duct and the resulting pressure drop between duct inlet and outlet. This interdepency is the underlying principle on which the actuator disk theory rests. Using the established approach to represent the action of a turbine blade by an actuator volume, the inertial resistance within that volume can be tuned to represent the thrust coefficient of a wind turbine [7]. The computed pressure drops and power extraction can be calibrated in terms of turbine blade motion and resulting torque to provide a translation from the CFD inertial resistance parameters to the actual device control. This calibration was completed through wind tunnel tests of a set of blades within the duct driving prototypes of the power takeoff.

With that calibration, the action of the airfoils in the ducts can be applied to a CFD model of the full device within a wider domain. At this stage that full domain was a virtual wind tunnel. Here the action of the airfoils extracting energy was to introduce a resistance of the approaching air to entering a duct. Too high a torque applied to the airfoil would result in too large a resistance, resulting in very little of the air passing into the duct and hence over the airfoils. Too low a torque would not utilise the energy of the air passing through the duct effectively. Hence, there is a range where the resistance is large enough to extract energy from the air but small enough to prevent all the air passing around the duct instead of through it. The key outcome of this set of calculations was a better understanding of this

balance between the duct capturing the air and the airfoils extracting the energy.

This will then provide a guidance for maximum power point control / best efficiency of the power train control in the next step of development beyond this study.

A. Single duct

The duct is a single section of a hexagon where the centre of the hexagon contains the shafts to which the aerofoils are attached. Its key dimensions are listed in Table I. For the calibration of the two actuator volumes, the fluid domain is exactly the space within the duct, using a uniform inlet velocity at the entry into the duct and a pressure outlet condition at the outlet.

Table I. – Key duct and device Characteristics

Parameter	Value	units
Duct length	2290	mm
Duct height	1135	mm
Sweep angle	55	°
Root radius of aerofoil	150	mm
Tip radius of aerofoil	750	mm
Blade length	600	mm
Blade chord	217	Mm
Airfoil: NACA0018 – 0016 – 0012		
Swept area	0.26	m^2
Location of first actuator volume centre from inlet	4660	mm
Location of second actuator volume	5225	mm
Actuator volume thickness	200	mm
Device height of 6 ducts	2271	mm
Frontal area of hex device	3.87	m^2

A schematic of the computational domain is shown in Figure 2, together with in indication of the computational mesh. Steady state solutions were computed for a range of inlet velocities from 10 m/s to 12 m/s and inertial resistance values from 2 m^{-1} to 10 m^{-1}. For the turbulence closure, the k-ω turbulence model was chosen.
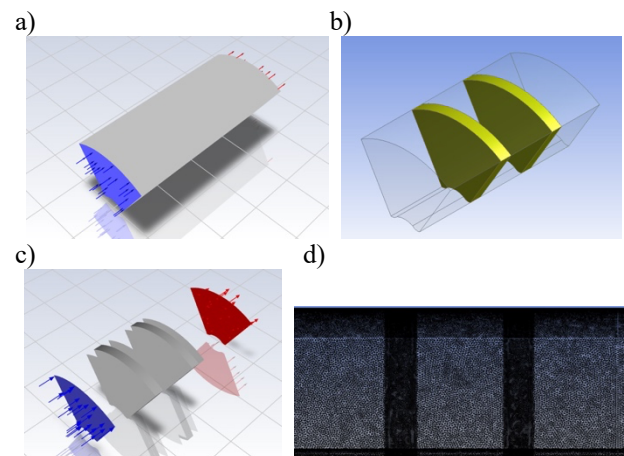

Fig.2. Computational domain for the individual duct.

Once a suitable range of inertial resistances had been determined, a 'hex' arrangement of 6 ducts, as shown in Fig. 3a, was placed on the ground of a virtual wind tunnel of length L= 14.6 m, width *W*= 10.5 m, and height *H*= 7.5 m, with the inlet to the ducts 6.1 m downstream of the inlet as shown in Figure 3b. Mesh convergence testing showed reliable results safely achieved with a little over 10 million elements (just under 2 million nodes)
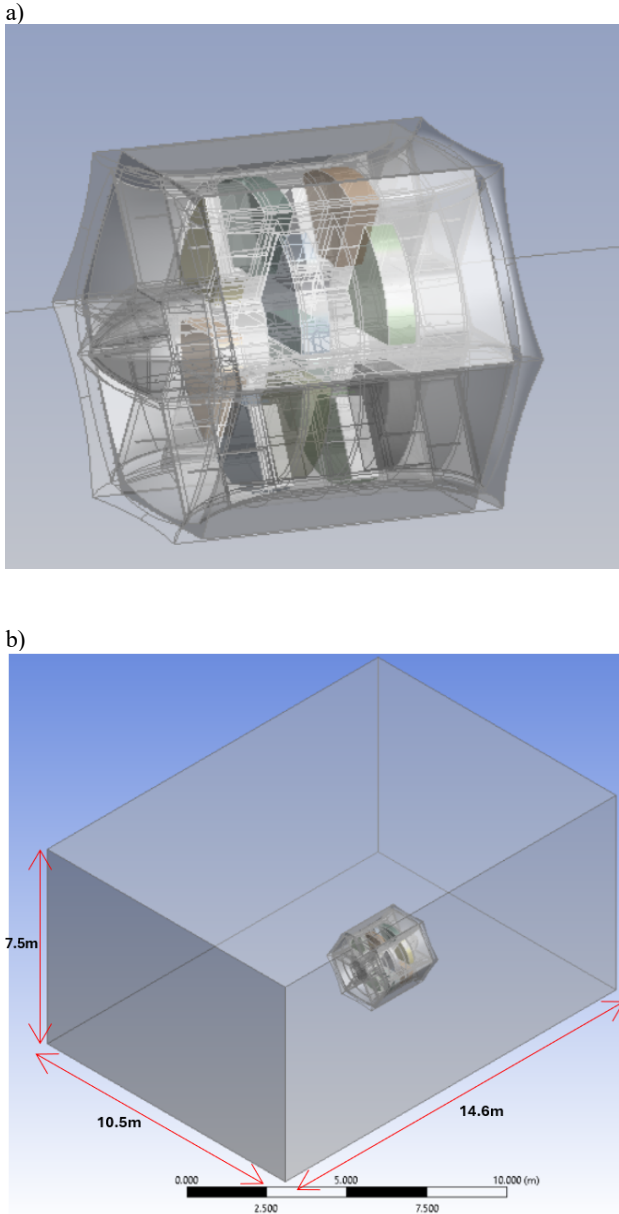
a)

b)

Fig.3. Computational domain for a full 'Hex' consisting of 6 ducts placed on the ground in a virtual wind tunnel .
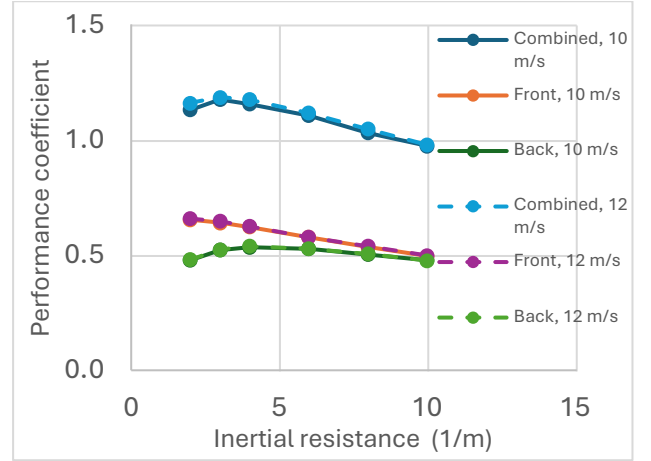

Fig.4. Performance coefficient for the individual actuator volumes (red in middle for front volume, green at bottom for rear volume, and top blue for the total duct.

3. Results

Following the Methodology, this section presents first the results of the single duct simulations and concludes with simulations of the full device in the virtual wind tunnel.

A. Single duct

The results from varying the tuning parameter, the inertial resistance on the power extraction of each of the two actuator volumes in the duct are shown in Fig. 4 as a performance coefficient for inlet wind speeds of 10 m/s and 12 m/s. The curves for the two wind speeds are virtually indistinguishable, with the bottom of the three for the second airfoil/actuator volume, the middle for the front airfoil, and the top for the set of the two airfoils combined. That coefficient is calculated like the efficiency of a wind turbine as

$$\Pi_P = \frac{P}{\frac{1}{2}\rho\,A\,U^3}$$

but, as Fig. 4 shows, exceeds 1 for the complete duct as the denominator does not take into account the pressure energy required to force the air through the duct against the energy extraction.

While the front actuator volume does not show any drop at the lowest inertial resistance value explored, the downstream actuator volume has a clear maximum at an intermediate value, resulting in an overall optimum performance at an inertial resistance of around 3 m^{-1}.

B. Full device in virtual wind tunnel

To test how the approaching air responds to the resistance caused by the energy conversion and how that flow might affect the flow through the separate ducts in the device, the complete device, referred to here as a 'Hex', was tested in the virtual wind tunnel for the same inlet wind speeds and inertial resistances as for the single duct.
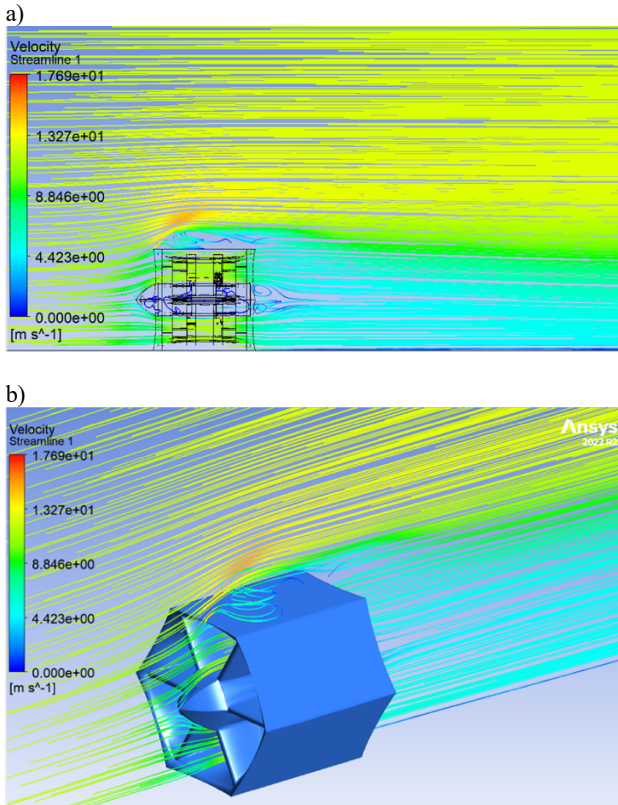
a)

b)

Fig.5. Flow fields in and around the device for inlet velocity 12 m/s and inertial resistance 3 m^{-1}.

a)

b)

Fig.6. Flow fields in and around the device for inlet velocity 12 m/s and inertial resistance 8 m^{-1}.

Figures 5 and 6 show velocity maps and streamlines for two example simulations, both for an inlet wind speed of 12 m/s, but Fig. 5 for an inertial resistance of 3 m^{-1}, near the best efficiency for the single ductc, and Fig. 6 for a much higher inertial resistance of 8 m^{-1}.

Both show the same general features: the approaching air is being partly deflected by the device. It shows a noticeable deceleration in front of the device, together with a significant acceleration over the device, including a recirculation area. Within the duct, the narrowing geometry from inlet to centre of duct leads to a speed-up. Both cases show a clear wake beind the device.

The main differences between the two is that the lower inertial resistance allows more of the air through the duct, leading to more effective conversion of the air's kinetic and pressure energy to power extraction. This also leads to a much more moderate wake behind the device compared to the case with the much higher inertial resistance. Tracing the streamline which just touches the top leading edge of the device, this originates from a height above ground approximately 85% of the total height for Fig. 5a but around 65% for Fig. 6a. This confirms that a key success requirement for the device will be careful tuning of the power take-off control to find the optimum of torque applied by the fluid to the airfoil while not presenting such a large resistance to the flow that the majority of the energy carrying air bypasses the device.
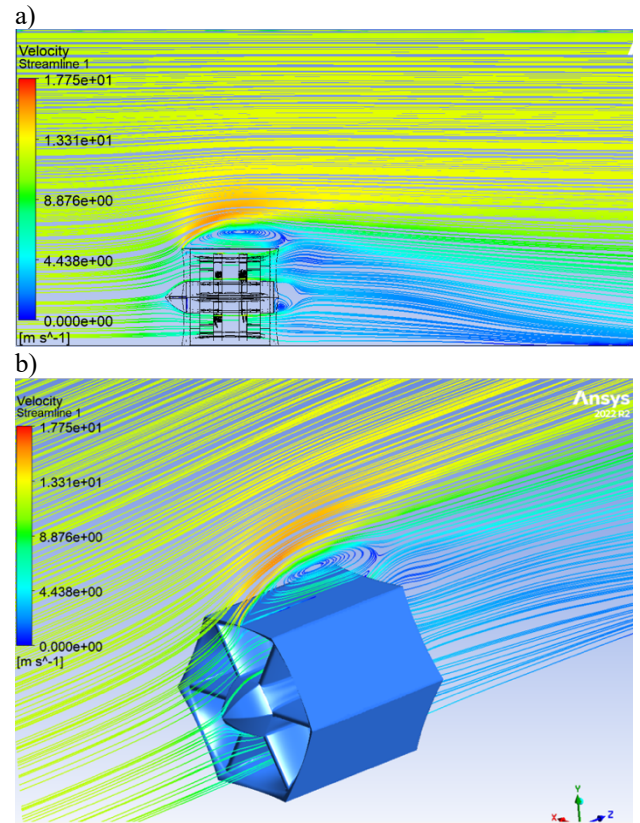
Progressing to the power extraction resulting from the simulated flow fields, the power output results, calculated as the pressure drops across the actuator volumes, are summarised in Table II. Here the upstream set of 6 airfoils is shown separately from the downstream set of airfoils, as well as the power output from the entire device.

Table II. – Analysis of average power from the full device at (a) 12 m/s and (b) 10 m/s for different inertial resistance values.

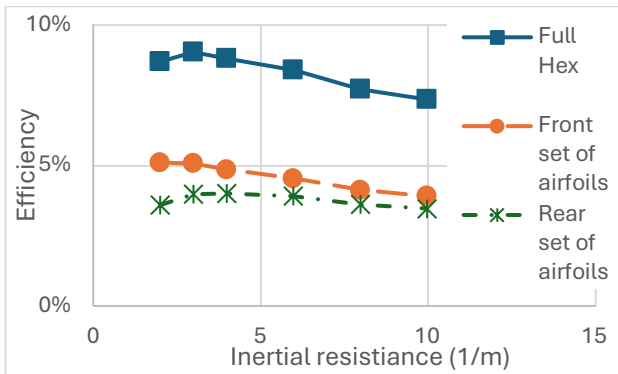| (a) Average Power - 6 ducts at 12 m/s			
Inertial Resistance (m^{-1})	Full duct (W)	1st set of aerofoils (W)	2nd set of aerofoils (W)
2	356	209	147
3	370	208	163
4	361	199	164
6	344	186	160
8	316	169	148
10	301	160	142
(b) Average Power (W) - 6 ducts at 10 m/s			
2	203	119	84
3	209	118	92
4	210	115	95
6	201	108	94
8	185	99	87
10	176	94	83

Fig.7. Efficiency for the full device (orange in middle for front set, green at bottom for rear set, and top blue for the total hex.

At a wind speed of 12 m/s, the maximum power output of 370 W was achieved at an inertial resistance of 3, whilst at 10 m/s, the peak power output of 210 W occurred at an inertial resistance of 4. This reduction in power at lower wind speeds aligns with the expected decrease in available kinetic energy for conversion. Based on the results for wind speeds of 10 and 12 m/s, the optimal inertial resistance is estimated to fall between 3 and 4, highlighting a critical range for maximising power extraction.

Figure 7 presents the results in terms of the device's efficiency, using the full frontal area of the device as the reference área, whereas the performance coefficient used in section 3.A only used the actual swept area of the oscillating airfoil. Compared to the simulations of the single duct showing performance coefficients for the pair of airfoils in excess of 1, here the optimum efficiency is between 9 % and 10 %. This significant difference is partly caused by the choice of reference area which includes the solid parts of the frontal area but also partly by the setting in the wind tunnel where the air is not forced through the duct but can bypass it to a degree given by the tuning of the power take-off.

4. Conclusion

The work presented here reports from a stage of the development of a novel wind energy converter targeted to be best suited for near-ground wind characterised by relatively low mean wind speeds but high turbulence. As such, the design target to capture small scale and short-lived eddies, the approach was to split the energy capture into sections using oscillating airfoils instead of sampling and averaging over a a full device/rotor diameter. One development task was to identify a suitable simulation tool to determined optimum control strategies and evaluate the device performance in the controlled environment of a wind tunnel.

The results demonstrate that the Wind Panel design is capable of harnessing wind energy to generate power. At wind speeds of 12 m/s, the design can extract up to 370 W, indicating strong performance under higher wind conditions. Even at lower wind speeds of 10 m/s, the system is able to produce 210 W, making it viable for a range of wind conditions. This shows that the Wind Panel design is versatile and efficient in converting wind energy into usable power. Ultimately, the design proves to be a reliable solution for sustainable energy production, capable of meeting power demands across varying wind speeds.

Having identified optimum conditions for the power train control to tune the resistance to the oscillating airfoils to mimic the optimum inertial resistance of 3 m^{-1}, one of the next steps in the device developments would be to evaluate how stacking a number of hex devices together could help to feed more air through such an assembly. Another development task would be to optimise the duct design to maximise air capture at the intake and minimise energy losses from the air during its passage through, and exit from the device ducts.

References

[1] A.D. Peacock et al., "Micro wind turbines in the UK domestic sector", Energy and Buildings (2008). Vol. 40, pp. 1324 – 1333. http://dx.doi.org/10.1016/j.enbuild.2007.12.004

[2] A. Bianchini et al, "Current status and grand challenges for small wind turbine technology", Wind Energy Science (2022). Vol. 7, pp. 2003-2037. https://doi.org/10.1016/j.ecmx.2023.100457

[3] A. Prévost et al., "A framework for technico-environmental optimization of small wind turbines", Applied Energy (2025). Vol. 377, 124502. https://doi.org/10.1016/j.apenergy.2024.124502

[4] W.-G. Früh, "Exploring technology options for future wind energy converters", Renewable Energy & Power Quality Journal (2024). Vol. 22. https://doi.org/10.52152/4062

[5] K. Calautit and C. Johnstone, "State-of-the-art review of micro to small-scale wind energy harvesting technologies for building integration", Energy Conversion and Management: X (2023). Vol. 20, 100457. https://doi.org/10.1016/j.ecmx.2023.100457

[6] Katrick Technologies Ltd, "Wind Panel", https://www.katricktechnologies.com/wind-technologies, accessed 11 Feb. 2025.

[7] A.C.W. Creech, W.-G. Früh and P. Clive, "Actuator volumes and hr-adaptive methods for three-dimensional simulation of wind turbine wakes and performance", Wind Energy (2012). Vol. 15, pp. 847-863. https://doi.org/10.1002/we.508